

Ferromagnetic polarons in $\text{La}_{0.5}\text{Ca}_{0.5}\text{MnO}_3$ and $\text{La}_{0.33}\text{Ca}_{0.67}\text{MnO}_3$

G. Zheng and C. H. Patterson

Department of Physics and Centre for Scientific Computation, University of Dublin, Trinity College, Dublin 2, Ireland

(Received 3 March 2003; published 18 June 2003)

Unrestricted Hartree-Fock calculations on $\text{La}_{1-x}\text{Ca}_x\text{MnO}_3$ ($x=0.5$ and $x=0.67$) in the full magnetic unit cell show that the magnetic ground states of these compounds consist of “ferromagnetic molecules” or polarons ordered in herring-bone patterns. Each polaron consists of either two or three Mn ions separated by O^- ions with a magnetic moment opposite to those of the Mn ions. Ferromagnetic coupling within the polarons is strong, while coupling between them is relatively weak. Magnetic moments on the Mn ions range between $3.8\mu_B$ and $3.9\mu_B$ in the $x=0.5$ compound and moments on the O^- ions are $-0.7\mu_B$. Each polaron has a net magnetic moment of $7.0\mu_B$, in a good agreement with recently reported magnetization measurements from electron microscopy. The polaronic nature of the electronic structure reported here is obviously related to the Zener polaron model recently proposed for $\text{Pr}_{0.60}\text{Ca}_{0.40}\text{MnO}_3$ on the basis of neutron-scattering data.

DOI: 10.1103/PhysRevB.67.220404

PACS number(s): 75.30.Et, 75.47.Lx, 71.27.+a, 75.10.-b

I. INTRODUCTION

The current paradigm for the electronic structure of manganites ($A_{1-x}B_x\text{MnO}_3$) with $x \geq 1/2$ is a lattice of Mn sites with d^3 or d^4 orbital occupancy, with the proportion of each decided by the value of x and orbital ordering (OO) of the occupied e_g orbital on d^4 sites. The corresponding double-exchange model Hamiltonian has been studied extensively.¹⁻³ Manganites with $x \geq 1/2$ usually exhibit a phase transition,⁴⁻⁹ which has been assumed to be charge ordering (CO) of the d^3 and d^4 sites at a temperature well below the paramagnetic transition temperature. The conventional picture of the orbital and charge ordered phase with the CE magnetic structure¹⁰ is shown schematically in Fig. 1(a).

The validity of this picture for the manganites has been questioned recently;¹¹⁻¹³ its contradictions were pointed out by Goodenough in 1955.¹⁴ An alternative picture, the Zener polaron,¹⁵ which challenges the ideas of double exchange and CO in the manganites, was recently proposed to account for the structure of $\text{Pr}_{0.60}\text{Ca}_{0.40}\text{MnO}_3$ determined by neutron scattering.¹⁶ In the conventional CO and OO picture, ordering of the e_g electron on d^4 Mn sites is expected to induce a Jahn-Teller (JT) distortion; the long Mn-O bond distance in LaMnO_3 exceeds 2.15 \AA ,^{10,17} while the Mn-O distance in cubic perovskite CaMnO_3 is 1.88 \AA .¹⁰ The lesser modulations of bond length in doped manganites with $x \sim 1/2$ (1.92 and 2.06 \AA in $\text{La}_{0.5}\text{Ca}_{0.5}\text{MnO}_3$ ⁵ and 1.98 and 2.01 \AA in $\text{Pr}_{0.60}\text{Ca}_{0.40}\text{MnO}_3$ ¹⁶) suggest an intermediate valence.

In this paper, we report results of unrestricted Hartree-Fock (UHF) calculations on $\text{La}_{1-x}\text{Ca}_x\text{MnO}_3$ for $x=1/2$ and $x=2/3$. The UHF electronic structure for these compounds is interpreted in terms of ferromagnetic polarons containing two ($x=1/2$) or three ($x=2/3$) Mn ions. The main difference between results from UHF calculations and the conventional double-exchange picture is that all Mn ions are essentially d^4 . Consequently, electrons must transfer from oxygen ions to every other Mn ion in the $x=1/2$ compound, resulting in an ordered array of O^- ions between pairs of Mn ions. The

structures of the polaron phases for $x=1/2$ and $x=2/3$ are shown schematically in Figs. 1(b) and 2.

Mn-O^- -Mn and Mn-O^- Mn-O⁻ Mn chains constitute the polarons for $x=1/2$ and $x=2/3$, respectively. Mn magnetic moments are in the range from $3.8\mu_B$ to $3.9\mu_B$ for either compound while oxygen ions within the polarons have charges closer to O^- than O^{2-} and magnetic moments of $-0.7\mu_B$. All other oxygen ions are essentially O^{2-} ions. Each polaron has net magnetic moment of $7.0\mu_B$, in good agreement with recently reported magnetization measurements from electron holography and Fresnel imaging.¹⁸

UHF calculations predict that magnetic coupling within polarons is strong and ferromagnetic (FM), while coupling between polarons is much weaker and can be antiferromagnetic (AF) or FM; these observations lead to a natural explanation for the observed CE or A-type AF magnetic ground states of manganites with $x=1/2$ (Refs. 4,8) and the magnetic ground state of $\text{La}_{0.33}\text{Ca}_{0.67}\text{MnO}_3$, which contains polarons with the magnetic moment roughly aligned along the polaron axis.⁶ Given that the magnetic coupling within the polarons is strong and FM, the appropriate model Hamiltonian for these systems at low temperature is a Heisenberg Hamiltonian on a triangular lattice where each polaron is a single magnetic entity, rather than the conventional double-exchange Hamiltonian.

Results of our UHF calculations are at odds with density-functional theory (DFT) calculations in the local spin-density approximation (LSDA) reported recently^{19,20} and with LSDA calculations done as a part of this work using the same electronic structure code²¹ in that UHF calculations predict a magnetic moment on oxygen ions within the polarons, where DFT calculations do not.

II. UHF CALCULATIONS

All electron UHF calculations were performed for $\text{La}_{0.5}\text{Ca}_{0.5}\text{MnO}_3$ and $\text{La}_{0.33}\text{Ca}_{0.67}\text{MnO}_3$ using the low-temperature structures refined using x-ray data by Radaelli and co-workers²² in the full (80 and 120 atom) magnetic unit cells.

Spin densities of $\text{La}_{0.5}\text{Ca}_{0.5}\text{MnO}_3$ (Fig. 3) and

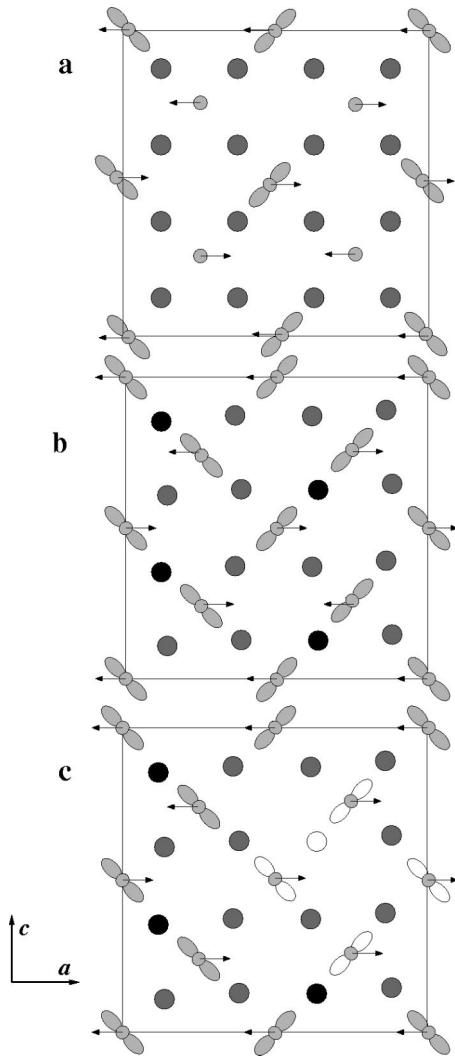


FIG. 1. Schematic illustrations of the magnetic unit cell for $A_{0.5}B_{0.5}MnO_3$ compounds with a CE magnetic structure: (a) the conventional double-exchange picture; (b) the polaronic picture; (c) a possible change in orbital order in a small ferromagnetic domain when an electron is added at the oxygen ion site indicated by an unshaded circle. Spins are indicated by arrows, Mn^{d^4} sites by double-lobed orbitals, Mn^{d^3} sites by small shaded circles, O^{2-} ions by larger shaded circles, and O^- ions by black circles.

$La_{0.33}Ca_{0.67}MnO_3$ (Fig. 4) in the ac planes of the crystal structures clearly show the polaronic nature of the electronic structures, including the magnetic moment of the O^- ions opposite to those of the neighboring Mn ions. The magnetic unit cells of either compound each contain four polarons in the ac planes shown.

Magnetic moments and Mulliken populations on Mn and oxygen ions in the polarons are given in Table I. Electron holography and Fresnel imaging¹⁸ measurements show that below the AF Néel temperature, the $x=1/2$ compound actually consists of both FM and AF domains, and that the magnetic moment per Mn ion in the FM domains was $(3.4 \pm 0.2)\mu_B$. UHF calculations predict a net magnetic moment of $7.0\mu_B$ for the polaron, i.e., the polarons are fully spin polarized, in agreement with these measurements of the mag-

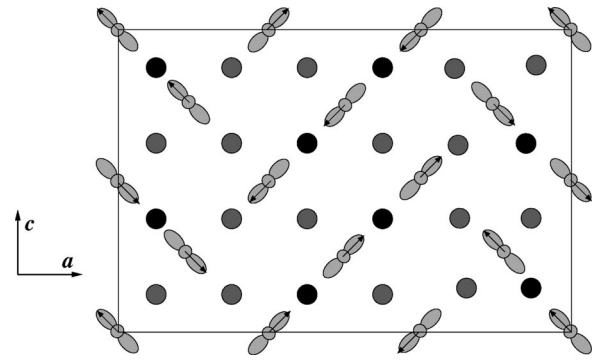


FIG. 2. Schematic illustration of the magnetic unit cell for $La_{0.33}Ca_{0.67}MnO_3$ with the experimentally observed magnetic structure. Spins are indicated by arrows, Mn^{d^4} sites by double-lobed orbitals, O^{2-} ions by shaded circles, and O^- ions by black circles.

netization of FM domains.¹⁸ Earlier neutron-scattering data for this compound (Table I) indicated magnetic moments somewhat smaller than these fully polarized values,⁵ but the trend, where larger moments are found on the sites denoted Mn^{3+} , is reproduced.

Mulliken populations from UHF calculations on $La_{1-x}Ca_xMnO_3$ indicate total Mn ion populations in the range from 2.25 ($x=0$) to 2.13 ($x=1$) with a monotonic variation for intermediate values of x . Mn d populations have an even smaller relative variation across the range of x with a d population of 4.66 in $LaMnO_3$, a range of d populations from 4.72 to 4.73 in $La_{0.5}Ca_{0.5}MnO_3$, and 4.70 in $CaMnO_3$. Similar d populations ($Mn^{3+}4.45$ and $Mn^{4+}4.36$) were found in model UHF calculations by Mizokawa and Fujimori.²³ The t_{2g} and e_g populations (with the z axis oriented along the Mn-Mn axis of a polaron) at the Mn^{3+} and Mn^{4+} sites were similar: $Mn^{3+} t_{2g}^{3.08} d_{3z^2-r^2}^{1.10} d_{x^2-y^2}^{0.55}$ $Mn^{4+} t_{2g}^{3.10} d_{3z^2-r^2}^{1.08} d_{x^2-y^2}^{0.55}$. The $d_{3z^2-r^2}$ orbitals are nearly fully spin polarized ($0.95\mu_B$ on both ion types), whereas the $d_{x^2-y^2}$ orbitals are weakly spin polarized. This is consistent with a bonding picture in which the t_{2g} shell on each Mn ion

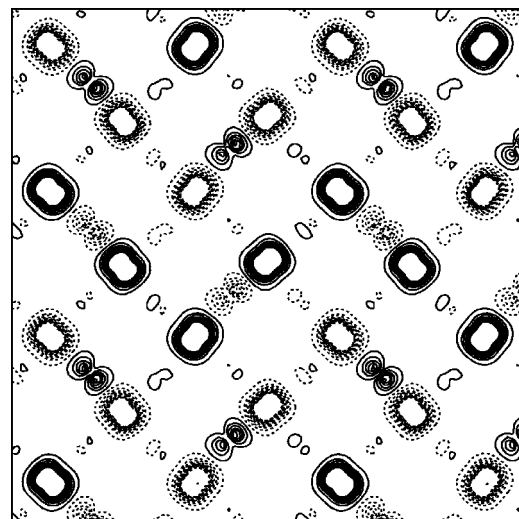


FIG. 3. UHF spin-density plot for $La_{0.5}Ca_{0.5}MnO_3$ in the CE-AF state.

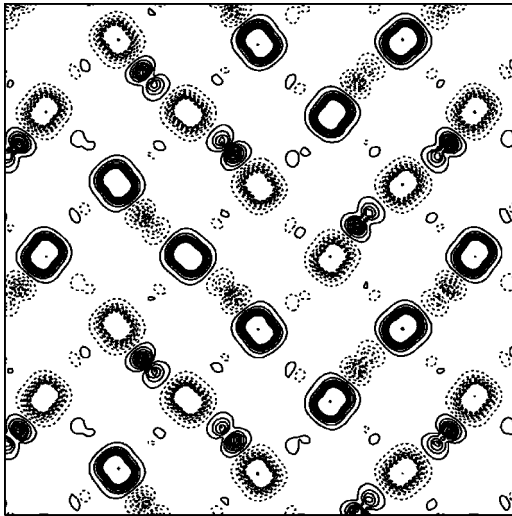


FIG. 4. UHF spin-density plot for $\text{La}_{0.33}\text{Ca}_{0.67}\text{MnO}_3$ in an FM state.

is half filled and a pair of e_g orbitals is combined with a set of four empty sp^3 orbitals to form a set of quasioctahedral d^2sp^3 hybrid orbitals for polar-covalent Mn-O bonding. The consistency of both the Mn ion population and d population across the range of values of x contradicts the conventional charge ordering picture where Mn ions are assumed to have their formal Mn^{3+} and Mn^{4+} charges.

Total energies were calculated for the FM state and four different low-energy AF states of the $x=1/2$ compound. Low-energy states are found by flipping entire polaron magnetic moments; flipping the spin of one of the Mn ions in a polaron results in an increase of the total energy by around 400 meV. Energies of the various low-energy magnetic states of the $x=1/2$ compound are well fitted by an Ising-like, nearest-neighbor Hamiltonian of the form given in Eq. (1). An Ising-like Hamiltonian has been used to fit the total energies for the various magnetic states of $\text{La}_{0.5}\text{Ca}_{0.5}\text{MnO}_3$, because UHF wave functions are eigenfunctions of the \hat{S}_z operator but are not eigenfunctions of the \hat{S}^2 operator. However, given the relative magnitudes of interpolaron and in-

TABLE I. Charges and magnetic moments in $\text{La}_{0.5}\text{Ca}_{0.5}\text{MnO}_3$ from Mulliken populations and experiment.

| | Mn moment (μ_B) | O moment (μ_B) |
|-----------------------------|-----------------------|----------------------|
| UHF (CE-AF) ^a | 3.91, 3.78 | -0.67 |
| UHF (CE-AF) ^{a, b} | 3.79, 3.65 | |
| Expt. ^{a, c} | 2.98, 2.57 | |
| Expt. ^d | 3.4 ± 0.2 | |
| | Mn charge | O charge |
| UHF (CE-AF) ^a | +2.18, +2.17 | -1.24 |

^aValues for the Mn moment at the Mn^{3+} and Mn^{4+} sites are quoted in that order.

^bModel Hamiltonian solved in the UHF approximation, Ref. 23.

^cNeutron scattering, Ref. 5.

^dElectron holography, value obtained for the FM domain per Mn ion, Ref. 18.

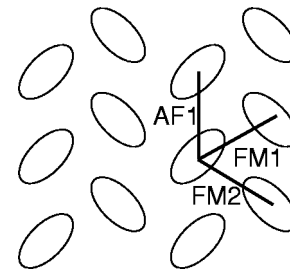


FIG. 5. Schematic illustration of exchange couplings between polarons in a Heisenberg Hamiltonian description.

trapolaron exchange couplings reported here, the appropriate Hamiltonian for a quantum simulation of the low-energy magnetic excitations of $\text{La}_{0.5}\text{Ca}_{0.5}\text{MnO}_3$ is a Heisenberg Hamiltonian with adjusted exchange constants.

$$H = \sum_{\langle ij \rangle} J_{ij} \frac{\hat{S}_{zi} \cdot \hat{S}_{zj}}{S^2}. \quad (1)$$

Labeling of exchange couplings is shown schematically in Fig. 5 and exchange constants obtained by fitting total energies of UHF calculations are given in Table II. The spin magnitude in Eq. (1) was chosen to be $S=2$.

Exchange couplings within the plane shown in Fig. 5 along zigzag chains are FM and roughly equal in magnitude, whereas these couplings are AF perpendicular to the zigzag chains. Exchange coupling between polarons in different type planes is AF. The magnetic ground state is expected to be CE type when J_{AF1} exceeds $(J_{FM1} + J_{FM2})/2$ in magnitude and A type otherwise. Both are observed to be the magnetic ground state for various $x=1/2$ compounds, depending on the A and B ion types⁸.

Our calculations actually predict an A type AF ground state, whereas the CE-AF structure is the ground state in $\text{La}_{0.5}\text{Ca}_{0.5}\text{MnO}_3$.¹⁰ However, in similar UHF calculations on LaMnO_3 ,²⁴ it was found that AF couplings are significantly underestimated compared to either experiment or results of configuration interaction (CI) cluster calculations, whereas FM couplings are in better agreement with both.

III. DISCUSSION

The polaronic picture for manganites with $x \geq 1/2$ which has been presented is consistent with a wide range of experimental data and allows various observations, such as the un-

TABLE II. Exchange coupling constants derived from $\text{La}_{0.5}\text{Ca}_{0.5}\text{MnO}_3$ UHF calculations.

| | Exchange constant (meV) |
|-------------|-------------------------|
| J_{AF1} | 5 |
| J_{AF2}^a | 8 |
| J_{FM1} | -14 |
| J_{FM2} | -12 |

^aAverage value over two interplanar couplings in crystallographic unit cell.

usual magnetization in $\text{La}_{0.33}\text{Ca}_{0.67}\text{MnO}_3$, to be explained. It accounts for the observation of A-AF or CE-AF ground states for various combinations of counterion in $\text{A}_{0.5}\text{B}_{0.5}\text{MnO}_3$;^{4,8} it is consistent with full spin polarization of Mn ions in $\text{La}_{0.5}\text{Ca}_{0.5}\text{MnO}_3$.¹⁸

One must be cautious in using UHF calculations to estimate magnitudes of magnetic moments on the oxygen ions. An analogy can be drawn between electron transfer from the O ion in a polaron to a neighboring Mn ion and separation of the electron pair in a hydrogen molecule as the proton-proton distance is increased above the molecular equilibrium bond length. UHF wave functions for hydrogen molecules at large bond distances consist of a spin-up electron on one proton and a spin-down electron on the other; the additional configuration in which spins on protons have been exchanged is omitted, owing to the simple functional form of the wave function. UHF (and LSDA) wave functions incorporate strong electron correlation effects at the cost of a proper treatment of electron spin. Spin symmetry is restored in CI methods, but these can only be applied to finite clusters owing to the large number of electronic configurations encountered in this approach. CI calculations on the pair of MnO_6 octahedra in the polaron in $\text{La}_{0.5}\text{Ca}_{0.5}\text{MnO}_3$ show that the overall spin configuration is a linear combination of several determinants²⁵ with a magnetic moment on the central oxygen ion. The $\text{La}_{0.5}\text{Ca}_{0.5}\text{MnO}_3$ polaron electronic structure therefore resembles that in $\alpha'\text{-NaV}_2\text{O}_5$;²⁶ it is unlike the electronic structure which results in the FM coupling in

LaMnO_3 , which is very well described by a single-spin configuration²⁴.

An obvious question which arises within the polaron picture is, “What happens when electrons are added to the $x = 1/2$ phase?” That is, “What is the electronic structure predicted to be in the FM region of the phase diagram with $0.2 < x < 0.5$?” Since the bottom of the conduction band in $\text{La}_{0.5}\text{Ca}_{0.5}\text{MnO}_3$ is comprised largely of vacant oxygen $2p$ states on the O^- ion in the polaron, one would naturally expect to add the extra electron here. The spin density plots in Figs. 3 and 4 show that OO in the $x = 1/2$ compounds is *parallel* to the polaron axis, whereas it is T-shaped in LaMnO_3 (long Mn-O bonds in JT distorted octahedra in LaMnO_3 are *perpendicular* to each other). If the extra electron is added to the polaronic oxygen site, it is expected that there will be reorientation of e_g orbitals [Fig. 1(c)] and adjustment of Mn-O-Mn bond lengths. The OO in the vicinity of the added electron is expected to resemble that in LaMnO_3 and one might expect to nucleate a small FM patch as further electrons are added.

ACKNOWLEDGMENTS

The authors wish to acknowledge discussions with W. Mackrodt, P.G. Radaelli, M. Towler, V. Ferrari, and P. Midgley. This work was supported by Enterprise Ireland under Grant No. SC/00/267 and by the Irish Higher Education Authority under the PRTLII-IITAC II program.

- ¹S. Yunoki, J. Hu, A.L. Malvezzi, A. Moreo, N. Furukawa, and E. Dagotto, *Phys. Rev. Lett.* **80**, 845 (1998).
- ²S. Fratini, D. Feinberg, and M. Grilli, *Eur. Phys. J. B* **22**, 157 (2001).
- ³E. Dagotto, T. Hotta, and A. Moreo, *Phys. Rep.* **344**, 1 (2001).
- ⁴H. Kawano, R. Kajimoto, H. Yoshizawa, Y. Tomioka, H. Kuwahara, and Y. Tokura, *Phys. Rev. Lett.* **78**, 4253 (1997).
- ⁵P.G. Radaelli, D.E. Cox, M. Marezio, and S.-W. Cheong, *Phys. Rev. B* **55**, 3015 (1997).
- ⁶P.G. Radaelli, D.E. Cox, L. Capogna, S.-W. Cheong, and M. Marezio, *Phys. Rev. B* **59**, 14 440 (1999).
- ⁷K.H. Kim, M. Uehara, and S.-W. Cheong, *Phys. Rev. B* **62**, R11 945 (2000).
- ⁸R. Kajimoto, H. Yoshizawa, Y. Tomioka, and Y. Tokura, *Phys. Rev. B* **66**, 180402 (2002).
- ⁹M. Pissas and G. Kallias, cond-mat/0205410 (unpublished).
- ¹⁰E.O. Wollan and W.C. Koehler, *Phys. Rev.* **100**, 545 (1955).
- ¹¹A.J. Millis, P.B. Littlewood, and B.I. Shraiman, *Phys. Rev. Lett.* **74**, 5144 (1995).
- ¹²G.M. Zhao, *Phys. Rev. B* **62**, 11 639 (2000).
- ¹³G.M. Zhao, Y.S. Wang, D.J. Kang, W. Prellier, M. Rajeswari, H. Keller, T. Venkatesan, C.W. Chu, and R.L. Greene, *Phys. Rev. B* **62**, R11 949 (2000).
- ¹⁴J.B. Goodenough, *Phys. Rev.* **100**, 564 (1955).
- ¹⁵D.I. Khomskii and G.A. Sawatsky, *Solid State Commun.* **102**, 87 (1997).
- ¹⁶A. Daoud-Aladine, J. Rodriguez-Carvajal, L. Pinsard-Gaudart, M.T. Fernandez-Diaz, and A. Revcolevschi, *Phys. Rev. Lett.* **89**, 097205 (2002).
- ¹⁷J. Rodriguez-Carvajal, M. Hennion, F. Moussa, A.H. Moudden, L. Pinsard, and A. Revcolevschi, *Phys. Rev. B* **57**, R3189 (1998).
- ¹⁸J.C. Loudon, N.D. Mathur, and P.A. Midgley, *Nature (London)* **420**, 797 (2002).
- ¹⁹Z. Popović and S. Satpathy, *Phys. Rev. Lett.* **88**, 197201 (2002).
- ²⁰J.E. Medvedeva, V. Anisimov, O.N. Mryasov, and A. Freeman, *J. Phys.: Condens. Matter* **14**, 4553 (2002).
- ²¹V.R. Saunders, R. Dovesi, C. Roetti, M. Caus’ a, N.M. Harrison, R. Orlando, and C.M. Zicovich-Wilson, *Crystal98 User’s Manual*, University of Torino, Torino, 1998. (www.cse.dl.ac.uk/Activity/CRYSTAL).
- ²²The $P21/m$ structure used for $\text{La}_{0.5}\text{Ca}_{0.5}\text{MnO}_3$ was obtained by x-ray diffraction at 20 K (Table I Ref. 5). The $Pnma$ Wigner crystal structure used for $\text{La}_{0.33}\text{Ca}_{0.67}\text{MnO}_3$ was obtained by powder neutron diffraction at 1.5 K (Table V of Ref. 6).
- ²³T. Mizokawa and A. Fujimori, *Phys. Rev. B* **56**, R493 (1997).
- ²⁴M. Nicastrò and C.H. Patterson, *Phys. Rev. B* **65**, 205111 (2002).
- ²⁵C.H. Patterson (unpublished).
- ²⁶N. Suaud and M.-B. Lepetit, *Phys. Rev. B* **62**, 402 (2000).